AIAA JOURNAL
Vol. 35, No. 9, September 1997

Studies of Low-Density Freejets and Their Impingement Effects

B. Deependran,* R. I. Sujith,† and Job Kurian‡
Indian Institute of Technology, Madras 600 036, India

A detailed experimental investigation of freejets and their impinging flowfields has been carried out. Studies were conducted for different pressure ratios, and the influence of Reynolds number on flow freezing was examined. A conical convergent–divergent nozzle of large area ratio, typically employed in aerospace applications, was used in the studies. Quantitative data of freejet and impingement flowfields, which could be used as a benchmark for checking the results obtained from numerical simulations such as the direct simulation Monte Carlo method, are presented. Forces due to plume impingement on an adjacent surface were estimated. The impingement effects were found to be considerable at high Reynolds numbers, whereas flowfield properties were found to be unaffected due to the presence of the plate at low Reynolds numbers. The freejet and the impinging flowfield were visualized using a glow discharge technique. The features of transition flow were observed in low Reynolds number flows. The flowfield modifications brought about by the influence of the flat plate could also be visualized.

Nomenclature

D_e = nozzle exit diameter
d^* = nozzle throat diameter
M = Mach number
P^* = pressure at throat
P_c = background pressure
P_f = Bird's freezing parameter
P_i = impact pressure
P_0 = stagnation pressure
r = radial distance from the center of expansion
T^* = temperature at throat
T_0 = stagnation temperature
U_e = flow velocity at nozzle exit
x = Cartesian coordinate along jet axis with origin at nozzle exit
y, z = Cartesian coordinates along the horizontal and vertical planes
z_0 = vertical distance of flat plate from jet axis, 10 mm
γ = ratio of specific heats for air, 1.4
λ^* = mean free path at throat
μ = coefficient of viscosity at T_0
ρ_e = flow density at nozzle exit
ω = temperature exponent of coefficient of viscosity, 0.75

I. Introduction

FREEJETS are employed in aerospace fields mostly as thrust generators. They find applications as thrusters in rockets and missiles, jet engines, satellite attitude control, stage separation, and orbit transfer, to name a few. They are also used in several nonaerospace fields, such as spray painting, gas welding, molecular beam generation, isotope separation, and lasers. Freejets from convergent–divergent (C–D) nozzles, encountered in many such applications, exhaust into low ambient pressures, making them highly underexpanded. Several of these applications also involve the impingement of the plume on some adjacent surface, inducing undesirable forces/torques, heat loads, contamination effects, etc. These undesirable forces/torques may not be considerable compared to the nozzle thrust. There are certain sensitive applications, however, as in the case of a satellite attitude control thruster, where the maneuver due to firing needs to be highly accurate so that it is capable of correcting very small disturbances, such as solar radiation, gas leakage, gravity acceleration, and impact of micrometeors. In some applications, the impingement area is very large, such as an adjacent stage of a stage separation thruster or some satellite component, as in an attitude control thruster. They may also be fired, though intermittently, over a long period of time. The cumulative undesirable effects will eventually reduce the mission life due to additional corrective firings undertaken. Thus, it is needless to stress the necessity of the study of low-density freejets from C–D nozzles and the evaluation of their undesirable effects due to impingement.

The nozzle flow expanding into low-density ambient conditions need not exhibit all of the features of a freejet in continuum flow.[1,2] Depending on the degree of rarefaction, the flow aerodynamics of a low-density freejet manifest differences, such as thickening of the shocks, large spreading of the plume, or nonexistence of shocks due to the freezing of the flow. The freezing of the flow happens because of the rapid decrease of density as the flow expands, reducing the intermolecular collision frequency. Once the collision frequency reduces, the interaction between the molecules is reduced, they can no longer establish local thermal equilibrium by collisional interaction, and, hence, the flow becomes frozen. In frozen flow, all flow properties attain limiting values despite a rapidly falling density. If the ambient is vacuum, the emanating flow is considered to be expanding radially like a source flow originating near the nozzle exit, without any shock system. Flow in the near field will be in continuum, but transition takes place as the streamline progresses into free molecular flow.[3] Even a freejet expanding into a low-density ambient faces breakdown of continuum flow and eventually becomes free molecular flow. In a study of breakdown of continuum flow, Bird[3] applied his empirical criterion to two-dimensional Prandtl–Meyer expansion and freejets expanding into vacuum. He suggested the value of a breakdown criterion, namely, Bird's freezing parameter $P_f = 0.05$. The usefulness of this criterion was verified by computation of the critical flow region using the direct simulation Monte Carlo (DSMC) method.[3]

Extensive study of low-density supersonic freejets issuing from sonic nozzles was undertaken by Anderson et al.[4] and Ashkenas and Sherman.[5] Ashkenas and Sherman give an account of the viscous effects on the flow structure. A numerical study of the effects of plume on structures far from the nozzle centerline was conducted by Boynton,[6] who predicted the large angle effects of fully developed laminar or turbulent boundary layers. An extension of this prediction was done by Simons.[7] In an experimental investigation, Legge et al.[8] analyzed the influence of the nozzle geometry, the nozzle boundary layer, and the ratio of specific heats on the plume density field. An experimental study by Dankert and Dettleff[9] on the near-field expansion in thrusters from C–D nozzles confirmed the existence of separate regions, i.e., an isentropic core and a boundary layer above a Reynolds number of 800. Chung et al.[10] numerically simulated an overexpanded low-density flow expanding through a C–D nozzle using the DSMC method and showed that the method can successfully predict Mach disk and barrel shocks.

Received June 6, 1996; revision received March 21, 1997; accepted for publication April 15, 1997.

*Senior Project Officer, Department of Aerospace Engineering.
†Assistant Professor, Department of Aerospace Engineering.
‡Associate Professor, Department of Aerospace Engineering.

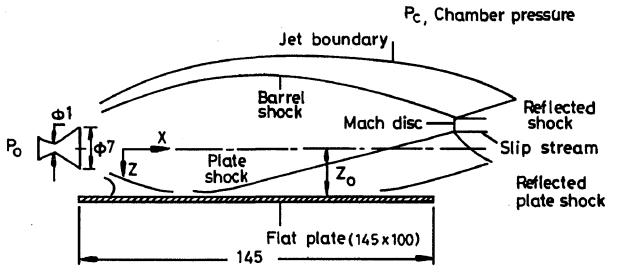

Fig. 1 Flowfield structure of freejet impingement. (All dimensions are in millimeters.)

Impingement effects pose serious problems in space flight. The interfering surface modifies the flowfield (as shown in Fig. 1). The size and shape of the Mach disk change. The plate shock is seen to emerge at the point at which the barrel shock interacts with the plate, and a second shock similar to the barrel shock can also be observed. A model for computing pressure and heat loads on adjacent surfaces near an underexpanded plume has been developed by Maddox.[11] Lengrand et al.[12] suggested semiempirical relations for the rapid estimation of jet characteristics and the dynamic effects of jet impingement. Allegre and Raffin[13] experimentally determined the heat transfer on the second and third stages of an Ariane launcher, as well as on its integrated payload during the separation of the second stage. Voznesensky et al.[14] experimentally estimated the heat and power loading distributions over a plate impinged upon by an underexpanded jet and also determined the form of the impingement shock wave. Legge and Boettcher[15] give an analytical model for prediction of the impingement forces on spacecraft structures. Calculation of the tangential and normal forces was performed by Allegre et al.[16] and Legge.[17,18] An in-depth study and review of plume flows and impingement effects is given by Dettleff.[19] Boyd et al.[20] performed numerical and experimental investigations to study low Reynolds number freejets and their impingement effects. They proved the usefulness of DSMC in predicting the flow characteristics of low-density expanding flows.

A survey of the literature reveals that exhaustive experimental studies of low-density freejets from C–D nozzles and the impingement effects have not been undertaken previously. In this background, an in-depth study was made of the entire flowfield of low-density freejets and impingement flowfield, both at similar flow conditions. This will aid in understanding the modifications to the freejet flowfield brought about by an adjacent surface. In addition, the data presented can be used as a benchmark for checking the results obtained from numerical simulations such as DSMC. The influence of Reynolds number on flow freezing of both the mentioned flowfields was also studied. A C–D nozzle typical of high-attitude applications was employed. A flat plate mounted parallel and off the plume axis simulated an adjacent surface. The nozzle and the flat plate were not changed for the various flow conditions to facilitate generalized understanding of the fluid dynamics. Quite a few studies have attempted to estimate the undesirable impingement forces using theoretical models or experimental determination by employing a balance setup. These undesirable impingement forces could be the normal force and the shear force on the impinged surface. They depend not only on the nozzle stagnation pressure, nozzle area ratio, throat area, nozzle divergence angle, plume spread, background pressure, etc., but also on the plate dimensions, its angle of attack, and the distance from nozzle axis. In this study an attempt is made to estimate the normal force on the plate by direct pressure measurements. The plate dimensions are chosen to contain the entire jet spread in the near field, where the impingement effects are expected to be considerable. In the far field, impingement effects are negligible because of the expansion of the jet to the ambient conditions.

II. Details of Experiments

The experiments were conducted in the Rarefied Gas Dynamics Facility of the Indian Institute of Technology, Madras. It is a contiguously run vacuum-pump-driven facility and essentially consists of a vacuum chamber, associated vacuum pumps, and flow-measuring instruments.

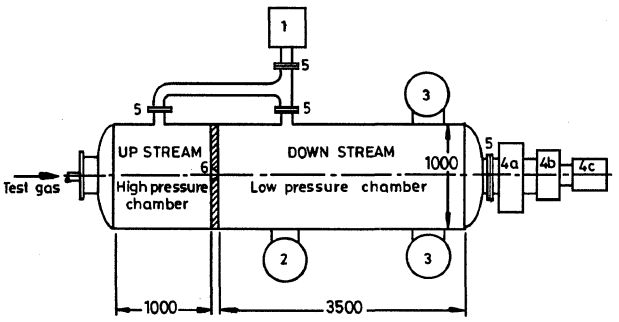

Fig. 2 Schematic of the test facility: 1, Ulvac rotary pump; 2, Edwards diffusion with backing pump; 3, Edwards booster pump; 4a, 4b, and 4c, Leybolds roots pump in three stages; 5, high vacuum valve; and 6, flow nozzle. (All dimensions are in millimeters.)

A. Facility Details

1. Vacuum Chamber

The vacuum chamber consists of a 4.5-m-long, 1-m-diam stainless-steel vessel, divided into two chambers by a partition flange (Fig. 2). The pumping system consists of mechanical pumps, a roots pump–trochoid pump combination, vapor booster pumps, and oil diffusion pumps, all of which together provide the desired vacuum in the chamber. The test gas from a high-pressure storage cylinder is leaked into the higher-pressure side of the chamber, from which it exhausts through the nozzle into the lower-pressure chamber. The conical C–D nozzle employed has an area ratio of 59.9 ($d^* = 1$ mm, nozzle divergence angle = 15.32 deg).

2. Pressure Transducers

Measurements of upstream, downstream, and impact pressure were made using capacitance-type MKS BARATRON pressure gauges. The appropriate range of the transducers was chosen, depending on the pressure values. The upstream chamber had a Wallace and Tiernan analog pressure manometer for high-pressure stagnation conditions, and the downstream chamber was fitted with a Pirani gauge. The downstream pressure from the MKS BARATRON gauge and the Pirani gauge were read simultaneously. These instruments have an accuracy of ±0.1% of reading, and the accuracy of the measured pressures is about ±1% for impact pressure and ±3% for chamber pressures.

3. Impact Pressure Probes

The impact pressure probe used here was the one introduced by Sankovich.[21] This probe does not require any correction for viscous or rarefaction effects, and its utility was well established by Raju et al.[22] in supersonic flows for the whole transition regime. Such an impact pressure probe was fabricated matching the dimensions of the plate and calibrated. The probe connected to the transducer was mounted in the vertical axis of a three-axis traverse mechanism, which could be remotely controlled with three counters, each unit having a least count of 0.01 mm.

4. Surface Pressure Measurements on Flat Plate

The plume impingement studies were performed by keeping a flat plate parallel to the plume axis. For this, a plate of dimensions 14.5 × 10 × 0.1 cm with its associated mounting arrangements was fabricated of aluminium. Another plate of dimensions 14.5 × 10 × 0.3 cm was fabricated for fixing thermistors for surface pressure measurements. Pressure taps of 0.75-mm diameter were drilled on the flat plate. On the side facing away from the flow, holes were drilled to suit the size of the thermistor to a depth of 2 mm (Fig. 3), which facilitates leak-proof fixing to the plates. Fixing was done using Araldite.

The normal pressure on the surface of the impinging plate was measured using thermistors as transducer. At low pressures, the temperature sensed by the thermistor directly corresponds to the surrounding pressure. This makes thermistors useful for measuring low pressures. Bead-type thermistors sealed in glass bulbs and manufactured by Fenwal Electronics were used.

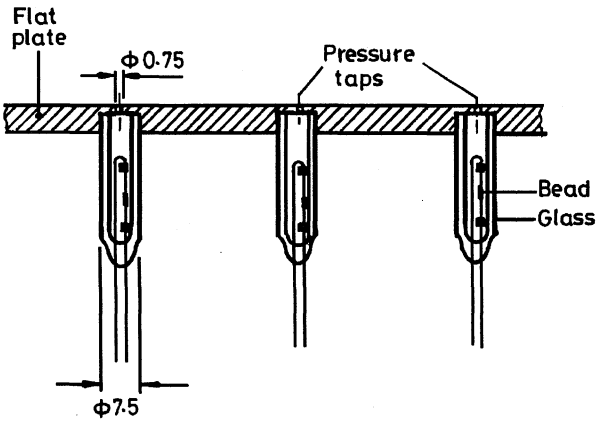

Fig. 3 Thermistor fixed to plate.

B. Experimental Procedure

A typical experimental run involved outgassing the tunnel for several hours until a minimum pressure of about 3×10^{-4} torr was maintained. The instruments were warmed up for the required duration. The storage cylinder containing dry air as the test gas was connected to the upstream region, and this was leaked into the chamber through a series of throttle and leak valves so that the upstream stagnation pressure could be maintained at the desired value. The gas exhausted through the nozzle into the downstream region and was evacuated by the pumps, which were continuously run. Measurements were performed only after the flow had stablized. For all flow conditions, the pressure maintained in the downstream section was the minimum possible, resulting from the exhaust through the nozzle and the constant evacuation by the pumps, and all of the experimental conditions could be repeated to a precision closer than ±1%. The pressure ratios maintained were between 10,000 and 20,000 so that all of the flow conditions were underexpanded.

III. Results and Discussion

A. Impact Pressure Surveys

1. Freejet Flowfields

Impact pressure measurements of underexpanded freejets from the same nozzle were performed at various pressure ratios and, hence, different Reynolds numbers. Reynolds number was calculated at the nozzle exit as

$$Re_e = \frac{\rho_e U_e D_e}{\mu}$$

For all of the cases, the stagnation temperature was found to be slightly below the atmospheric temperature. Change in viscosity due to small changes in temperature was neglected and, hence, in all cases the viscosity considered was that at 25°C. Both low and high Reynolds number flows were investigated. A parameter called Bird's freezing parameter, P_f, as defined in Ref. 3, was used to identify the continuum flow from the frozen flow:

$$P_f = \sqrt{\frac{\gamma\pi}{2}}\frac{\sqrt{M^2-1}}{\gamma+1}\left\{\frac{\{1+[(\gamma-1)/2]M^2\}}{[(\gamma+1)/2]}\right\}^{[1/(\gamma-1)]-\omega+\frac{1}{2}}\frac{\lambda^*}{\gamma}$$

$$\lambda^* = \frac{16\mu(T_e)}{5P^*}\sqrt{\frac{RT^*}{2\pi}}$$

Bird's freezing parameter $P_f = 0.05$ is taken as the value at which continuum breakdown occurs. A well-defined shock structure can be established only if the flow is in continuum. As a result, a Mach disk does not appear if the flow gets frozen before the location of the Mach disk is reached. The details of flowfield conditions, i.e., stagnation pressure, pressure ratio, ambient pressure, Reynolds number, and freezing parameter P_f, under which the various experiments were conducted are given in Table 1.

Impact pressure measurements were performed by moving the probe mounted on the traversing mechanism. For a particular pressure ratio, pressure surveys were conducted axially and at different axial locations in the cross plane. The axial direction is denoted as the x axis, and the horizontal cross plane is denoted as the y axis. The cross plane perpendicular to the y axis in the vertical direction is defined as the z plane. The flow is considered to be isentropic in the core region. Knowing the impact pressure and stagnation pressures, Mach numbers are calculated using the normal shock equation for the ratio of total pressures. For these experiments, the pressure ratios range from 10,000 to 20,000 and Reynolds number from 10 to 1000. Hence, the influence of Reynolds number on the jet structure and flow freezing could be ascertained. The variation of normalized pressures (P_i/P_0) with normalized distances (x/d^*) for various pressure ratios is shown in Fig. 4, which shows P_i/P_0 to be very high at the nozzle exit and decaying very fast downstream to the ambient pressure. Therefore, it can be concluded that the expansion process is very rapid in the near-field flow and thereafter gradual. The lower impact pressure sensed by the probe downstream implies that the shock ahead of the probe has occurred at a higher

Table 1 Range of flow variables of the experiments

Stagnation pressure P_0, torr	Ambient pressure P_c, torr	Pressure ratio P_0/P_c	Reynolds no. Re	Freezing parameter, P_f	Remarks
6	6×10^{-4}	10,000	13	1.93	
15	1.099×10^{-3}	13,650	33	0.77	Frozen
30	1.802×10^{-3}	16,650	67	0.39	
100	5×10^{-3}	20,000	222	0.025	Continuum
200	1.099×10^{-4}	18,200	444	0.012	in
300	1.72×10^{-2}	17,450	666	0.008	near field
450	2.47×10^{-2}	17,500	1,000	0.0055	

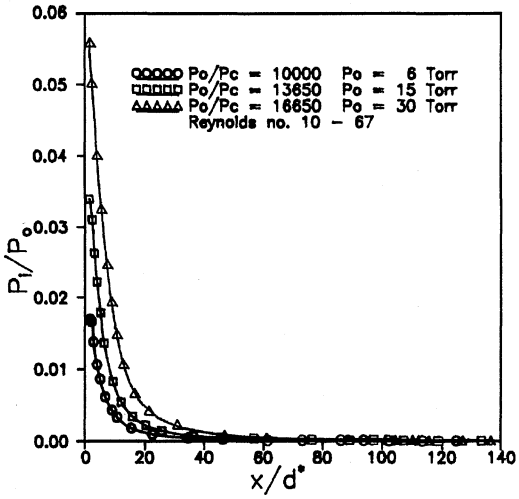

a) Low Reynolds number flows

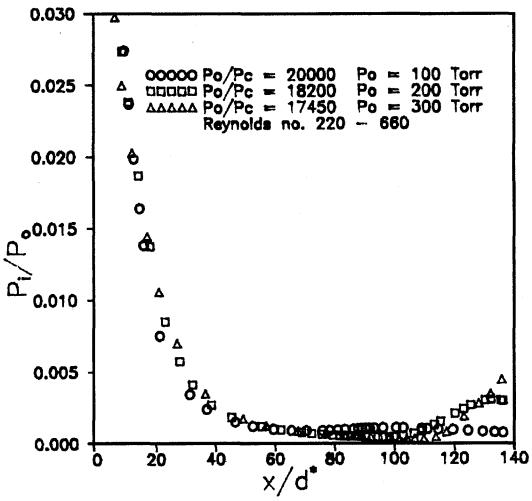

b) High Reynolds number flows

Fig. 4 Axial pressure distribution of a freejet.

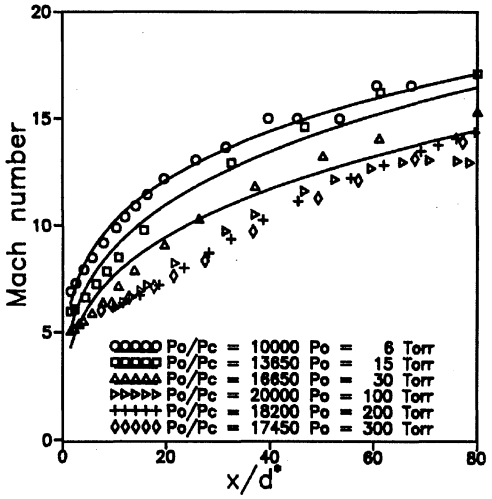

Fig. 5 Mach number along the axis of the freejet.

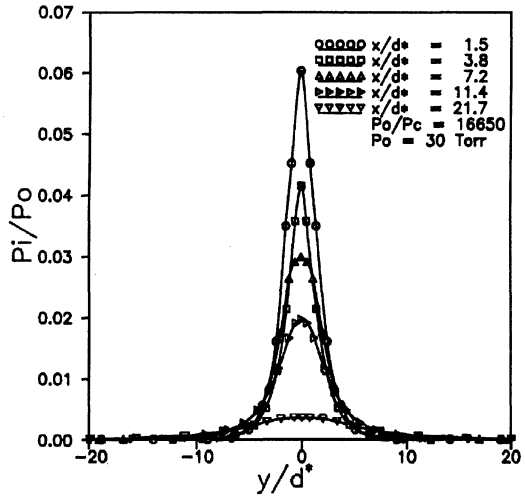

Fig. 6 Cross-plane pressure distribution.

Mach number and that the Mach number of the flow increases progressively downstream (Fig. 5).The slow rate of increase of Mach number at larger x locations is indicative of the flow velocity nearing maximum adiabatic limit and the temperature remaining less affected due to expansion because of fewer collisions.

A similar trend of sudden reduction in measured impact pressures away from the axis is shown by the cross-plane pressure profiles in Fig. 6. The rate of fall of impact pressure is steeper in the near-field regions and more gradual downstream because the flow has already expanded. Plots of constant pitot pressures in one axial plane (Fig. 7) give a good picture of the expansion process. The impact pressure surveys do not indicate the presence of any shocks in the flowfield for lower Reynolds number flows ($Re \leq 200$), suggesting that the flow may be frozen right from the nozzle exit.

In the high Reynolds number flows ($Re \geq 200$), however, pressure profiles do indicate the presence of shocks in the flowfield. The axial pressure profile initially falls rapidly, indicating a sudden expansion. Farther downstream, the measured impact pressures start increasing at a location depending on pressure ratio. This was found to be the location at which the barrel shocks interact with each other. The increase in measured pressure is a result of the momentum transfer taking place due to the flow structure there. A careful examination of the flowfield, as seen from glow discharge visualization photographs, reveals that the geometry of the barrel shock just before interaction is such that the barrel shocks, which are essentially oblique shocks, turn the surrounding flow toward the axis, incurring a momentum transfer toward the axis. The resulting momentum increase to the axial flow is sensed as an increase in stagnation pressure by the probe stationed there. This pressure rise diffuses off downstream due to flow expansion (as shown by the trends in Fig. 4b). It can also be ascertained that the size of the first

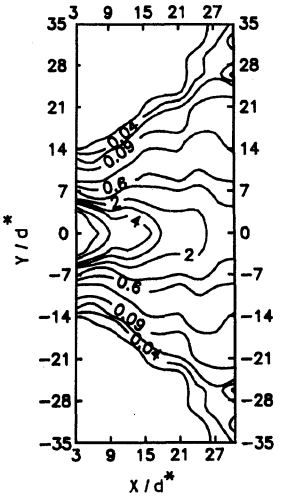

Fig. 7 Isopitot pressure lines in the cross plane of a freejet; $P_0/P_c = 17{,}450$, $P_0 = 300$ torr.

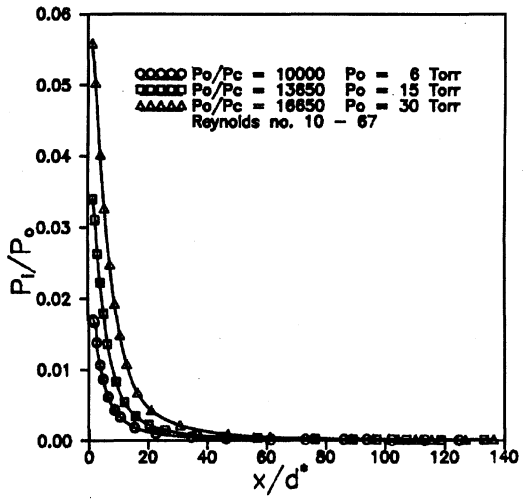

a) Low Reynolds number flows

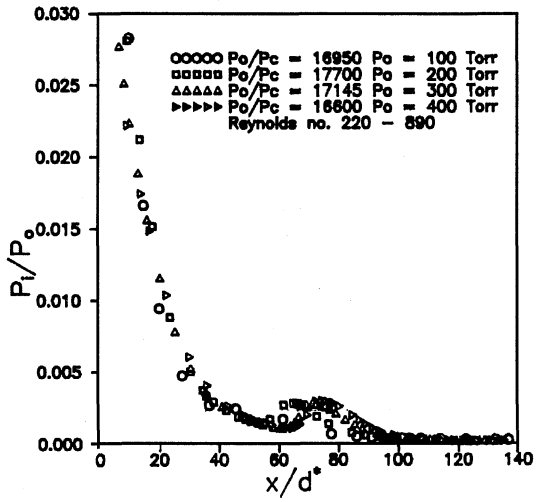

b) High Reynolds number flows

Fig. 8 Axial pressure distribution of a freejet impinging on a flate plate.

shock cell increases with the pressure ratio, as reported by Love et al.[1]

2. Impingement Flowfield Studies

For plume impingement studies, a flat plate was mounted parallel to the nozzle axis at a distance $z_0 = 10$ mm from the nozzle axis. As in the earlier experiments, axial (Fig. 8) and cross-plane pressure surveys were performed, and the influence of Reynolds number on flow freezing was addressed. In addition, the impact pressure

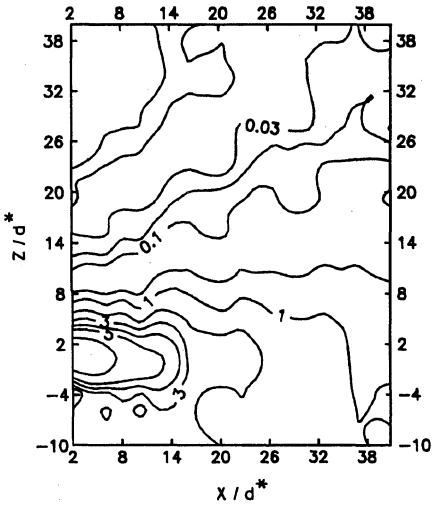

Fig. 9 Isopitot pressure lines in the cross plane (z plane) of a freejet impinging on a flate plate, 10 mm below the nozzle axis; P_0/P_c = 17,450, P_0 = 300 torr.

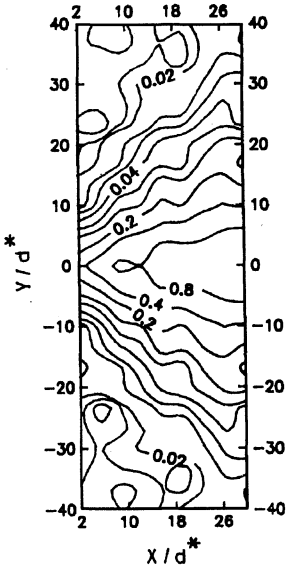

Fig. 10 Isopitot pressure lines on the surface of the plate; P_0/P_c = 17,450, P_0 = 300 torr.

measurements over the surface of the plate and cross-plane pressure measurements in the asymmetric plane (z plane) were also conducted. The influence of the plate on the flowfield can be understood from the plot of isopitot pressure lines in the z plane in Fig. 9. The plate confines expansion in the cross plane in the near field. But in the far field, pitot pressure field is not significantly altered. The plot of isopitot pressure lines on the surface of the plate in Fig. 10 gives information regarding the extent of plume spreading. Knowledge of plume spread, especially in the near field, could aid in modeling control thrusters for minimum impingement effects. Higher pitot pressures appear a little downstream on the plate surface, and the rate of the lateral expansion could be ascertained. The axial pressure distributions for freejets and impinging flowfields are compared in Fig. 11. Figure 12 shows maximum impingement pressure on the surface of the plate. The location of maximum impingement pressure on the surface of the plate for each pressure ratio is found to shift downstream with increasing stagnation pressure, implying that the flow becomes less divergent with increasing stagnation pressure and, hence, Reynolds number. This substantiates the observation by Dankert et al.[9] that, for $Re \geq 800$, a thick boundary layer comes into being, resulting in the flow becoming less divergent.

For low Reynolds number flows, impact pressure surveys of the impinging flowfield did not show much influence of the presence of the flat plate (Fig. 11). Because the flow was frozen, it was not surprising that pressure profiles did not give any indication regarding the presence of shock waves. Examination of the axial pressure profiles for high Reynolds number flows shows the same characteristics

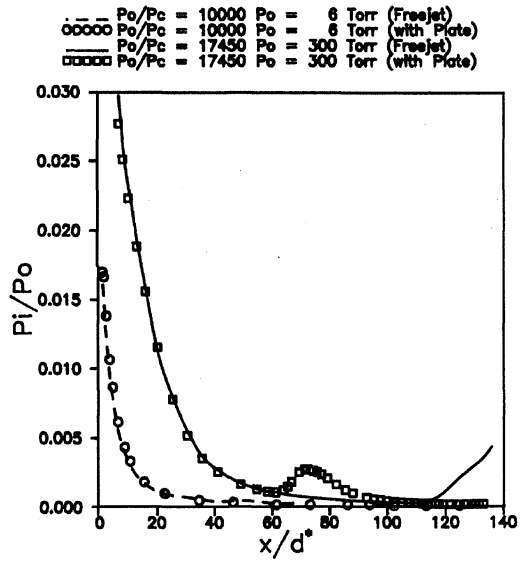

Fig. 11 Comparison of axial pressure distribution for a freejet and an impinging flowfield.

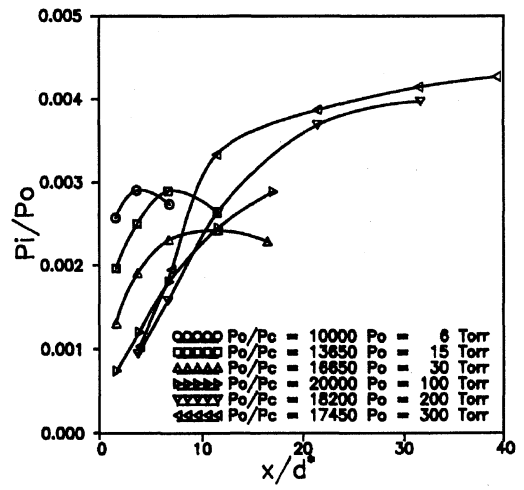

Fig. 12 Location of maximum impingement pressure on the plate surface.

of expansion in the near field of the nozzle as in an underexpanded freejet. However, there is an increase in impact pressure downstream, and this occurs ahead of the location where a similar pressure rise was observed for the corresponding freejet (see Figs. 4b, 8b, and 11). This pressure rise is attributed to the plate shock crossing the axis ahead of the location of the Mach disk (compare Figs. 14 and 15b). Farther downstream this increase in pressure diffuses due to the expansion process. The cross-plane pressure surveys in both the y and z directions also show the sudden radial expansion near the jet axis and the flow asymmetry brought about by the presence of the flat plate.

B. Surface Pressure Measurements

Surface pressure measurements on the impinged plate were performed using thermistors. These measurements facilitate the calculation of the force normal to the plate. Measurements were performed for both low and high Reynolds number flows from an underexpanded freejet. The pressure ratios and stagnation conditions were maintained the same as in the impact pressure studies of underexpanded freejets (see Table 1). The isobars for the surface pressure distribution are plotted in Fig. 13. These isobars give a glimpse of the relative pressure distributions on the impinged plate. The pressure distribution depends, first, on the freejet plume shape and also on the location of the plate shock, which in turn is governed by various parameters, such as the pressure ratio, plate distance, and nozzle

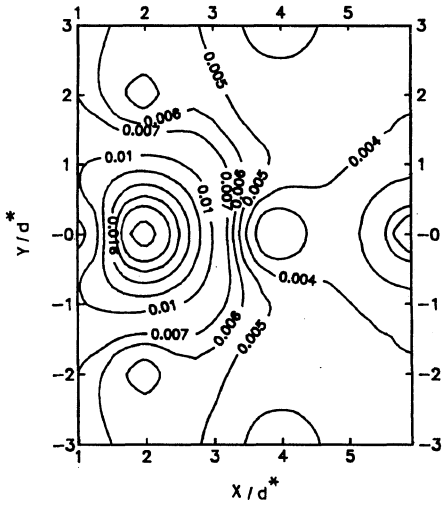

a) Low Reynolds number; P_0/P_c = 10,000, P_0 = 6 torr

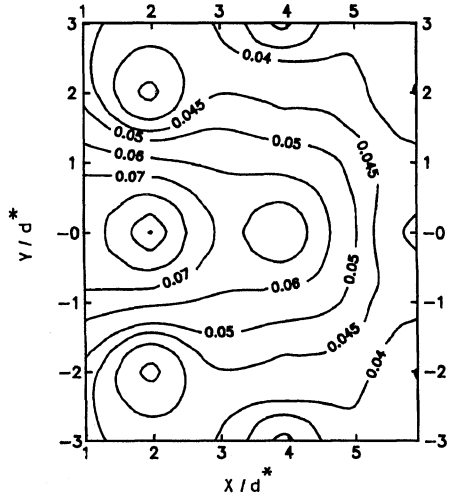

b) High Reynolds number; P_0/P_c = 17,500, P_0 = 450 torr

Fig. 13 Isobars on the plate surface.

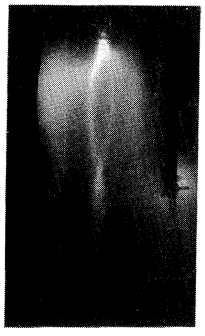

Fig. 14 Glow discharge photograph of a freejet in continuum flow (flow from top to bottom).

divergence angle. A characteristic difference in the plot of the isobars between frozen and continuum flows can be seen. In the frozen flow case (Fig. 13a), normal pressures are higher near the nozzle exit. But in the continuum case (Fig. 13b), higher values of normal pressure extend downstream of the plate. This is because, in addition to the plume getting less divergent with high Reynolds numbers, the plate shock that exists in high Reynolds number flows (continuum flow) modifies the flowfield over the plate. On the other hand, in frozen flows the plume expands like a source flow from the nozzle exit.

The normal force acting on the plate is calculated from the plot of the isobars. This is done by summing the product of the average force between two isobars with the surrounded area. The forces calculated vary from 0.0045 N (Re = 12) to 0.078 N (Re = 800).

The methodology proposed by Legge and Boettcher[15] for calculating the shear force was used. Essentially, they extracted simple

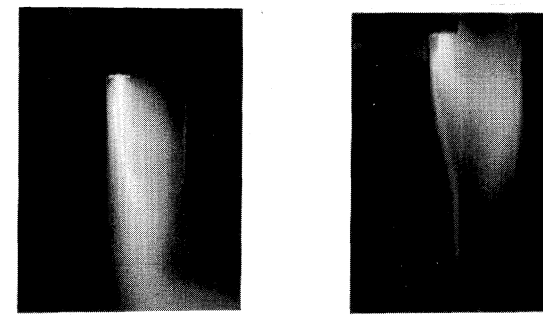

a) Frozen flow b) Continuum flow

Fig. 15 Glow discharge photograph of a freejet impinging on a flat plate (flow from top to bottom).

models from previous analytical and numerical work and used them to calculate forces and moments on spacecraft surfaces. From the set of equations as given by Legge,[17] the shear stress distributions are determined. Shear stress is considered to act only at locations covered by the plume, given by the impact pressure measurements on the plate surface in Fig. 10. The calculated shear force varied from 6×10^{-6} N (Re = 12) to 2.3×10^{-3} N (Re = 800). The thrust generated by the nozzle varied from to 1×10^{-3} N (Re = 12) to 6×10^{-2} N (Re = 800). Because the relative magnitudes of these undesirable forces are considerable, especially at high Reynolds numbers, their presence will negatively influence the jet–surface interactions. The normal force, which is a strong function of plate dimensions, was seen to easily overshoot the magnitude of thrust levels for the present configuration of experiments. In contrast, shear force levels were found to be only a maximum 4% of the nozzle thrust in the most severe case.

C. Glow Discharge Flow Visualization

The flowfields were visualized using glow discharge.[23] The pressure ratios and Reynolds numbers were the same as in the study of freejets and impingement flowfield. Figure 14 is a photograph of a typical freejet in a low-density continuum flow. This high Reynolds number flow does show the existence of the first shock cell. Farther downstream, the shock system is not seen. This must be because of the possibility that a clear shock system cannot be established downstream due to flow getting gradually frozen with the expansion. The barrel shocks are seen to curl back toward the plume axis and intersect at the axis and thereupon are seen to reflect downstream. Increase in pressure ratio increases the size of the shock cell, and the shock structure is seen to grow more distinct with increasing stagnation pressure as the flow becomes more continuum.

In the impingement flowfield of a low Reynolds number flow (Fig. 15a), where flow is calculated to be frozen, no shock structure is seen despite the flow being highly underexpanded. This confirms the frozen flow behavior of low Reynolds number flows. The impingement flowfield picture of high Reynolds number flow (Fig. 15b) clearly shows the plate shock emerging from the location where the barrel shock intersects the plate. The plate shock modifies the flowfield and is seen to intersect with the top barrel shock. Downstream, the two shocks move coincidentally as a dense flow region. The reason is that the incident angles at the intersection are such that the reflected shocks are nearly parallel to each other. No information about the flowfield over the plate downstream of the plate shock could be obtained. The pressure at the plate surface after the plate shock will depend on the location of the plate shock and the shock angle. The plate shock angle in turn will adjust itself so that flow over the plate is parallel to the plate boundary. The plate shock location is decided by the shape of the barrel shock and, hence, the pressure ratio. This also implies that the pressure distribution over the plate surface is dependent on the nozzle pressure ratio, exit Mach number, and flow angle at the location where the plate shock originates.

IV. Conclusions

An experimental investigation of low-density freejets issuing from a conical C–D nozzle and their impingement flowfield was

undertaken. Quantitative data of both the flowfields are presented. Impact pressure measurements of freejets and impinging flowfields confirm the absence of a well-defined shock system for low Reynolds number (frozen) flows. This is because a well-defined shock system can exist only in a continuum flow. Measurements give indications of flow expansion, similar to a source flowfield. Studies also show conclusively that expansion is very sudden in the near-field flow of nozzles. The expansion rate in the radial direction from the plume axis shows similar trends. The asymmetry in impact pressure measurements due to the influence of the adjacent surface is minimal for low Reynolds number flows, except near the plate surface, whereas the plate significantly modifies the flowfield at high Reynolds numbers. Shear stress calculations reveal that impingement effects are negligible at low Reynolds numbers ($Re \leq 200$) but are comparable to the nozzle thrust at high Reynolds numbers ($Re \geq 200$). The normal force on the plate is considerable compared to nozzle thrust in all flow regimes. Glow discharge visualization further validates the nonexistence of shocks in frozen flow. The shock structure of the impingement flowfield is understood fairly well and corroborates the features noted by measurements.

Acknowledgments

The experiments were conducted as part of the research project titled "Studies on Plume Flows and Plume Impingement" sponsored by the Indian Space Research Organisation. The authors would like to acknowledge the help given by A. R. Srikrishnan and also the commendable expertise of John George, Senior Scientific Officer, and Nallaperumal Pillai, Supervisor of the Rarefied Gas Dynamics Laboratory, Indian Institute of Technology, Madras, in this work.

References

[1]Love, E. S., Grigsby, C. E., and Lee, L. P., "Experimental and Theoretical Studies of Axisymmetric Freejets," NASA TR R-6, 1959.

[2]Adamson, T. C., and Nicholls, J. A., "On the Structure of Jets from Highly Under-Expanded Nozzles into Still Air," *Journal of the Aeronautical Sciences*, Vol. 26, Jan. 1959, pp. 16–24.

[3]Bird, G. A., "Breakdown of Continuum Flow in Freejets and Rocket Plumes," *Rarefied Gas Dynamics*, edited by S. S. Fisher, Vol. 74, Progress in Astronautics and Aeronautics, AIAA, New York, 1980, pp. 681–694.

[4]Anderson, J. B., Andres, R. P., Fenn, J. B., and Maise, G., "Studies of Low Density Supersonic Jets," *Rarefied Gas Dynamics*, edited by J. H. de Leeuw, Vol. 2, Advances in Applied Mechanics, Academic, New York, 1964, pp. 106–127.

[5]Ashkenas, H., and Sherman, F. H., "The Structure and Utilization of Supersonic Freejets in Low Density Wind Tunnels," *Rarefied Gas Dynamics*, edited by J. H. de Leeuw, Vol. 2, Advances in Applied Mechanics, Academic, New York, 1964, pp. 84–105.

[6]Boynton, F. P., "Exhaust Plumes from Nozzles with Wall Boundary Layers," *Journal of Spacecrafts and Rockets*, Vol. 5, No. 10, 1968, pp. 1143–1147.

[7]Simons, G. A., "Effect of Nozzle Exhaust Boundary Layers on Rocket Exhaust Plumes," *AIAA Journal*, Vol. 10, No. 11, 1972, pp. 1534, 1535.

[8]Legge, H., Dankert, C., and Dettleff, G., "Experimental Analysis of Plume Flow from Small Thrusters," *Rarefied Gas Dynamics*, edited by H. Oguchi, Vol. 1, Univ. of Tokyo Press, Tokyo, Japan, 1984, pp. 279–288.

[9]Dankert, C., and Dettleff, G., "Near-Field Expansion in Thruster Plumes," *Rarefied Gas Dynamics*, edited by A. E. Beylich, VCH, Aachen, Germany, 1990, pp. 1003–1010.

[10]Chung, C. H., De Witt, K. J., Stubbs, R. M., and Penko, P. F., "Simulation of Overexpanded Low-Density Nozzle Plume Flow," *AIAA Journal*, Vol. 33, No. 9, 1995, pp. 1646–1650.

[11]Maddox, A. R., "Impingement of Underexpanded Plumes on Adjacent Surfaces," *Journal of Spacecrafts and Rockets*, Vol. 5, No. 6, 1968, pp. 718–724.

[12]Lengrand, J. C., Allegre, J., and Raffin, M., "Underexpanded Freejets and Their Interaction with Adjacent Surfaces," *AIAA Journal*, Vol. 20, No. 1, 1982, pp. 27, 28.

[13]Allegre, J., and Raffin, M., "Experimental Study of Plume Impingement and Heating Effect," *Rarefield Gas Dynamics*, 13th International Symposium on Rarefied Gas Dynamics, edited by O. M. Belotserkovskii, M. N. Kogan, S. S. Kutateladze, and A. K. Rebrov, Vol. 2, Plenum, New York, 1985, pp. 965–974.

[14]Voznesensky, E. N., Nemchenko, V. I., and Sokhatsky, A. V., "Some Peculiarities of Power and Heat Interaction of a Low Density Highly Under-Expanded Jet with a Flat Plate," *Rarefied Gas Dynamics*, 13th International Symposium on Rarefied Gas Dynamics, edited by O. M. Belotserkovskii, M. N. Kogan, S. S. Kutateladze, and A. K. Rebrov, Vol. 2, Plenum, New York, 1985, pp. 1001–1008.

[15]Legge, H., and Boettcher, R. D., "Modelling Control Thruster Plume Flow and Impingement," TR, DLR Inst. for Experimental Fluid Mechanics, Göttingen, Germany, 1982.

[16]Allegre, J., Raffin, M., and Lengrand, J. C., "Forces Induced by Simulated Exhaust Plume Impinging upon a Flat Plate," *Rarefied Gas Dynamics*, edited by H. Oguchi, Vol. 1, Univ. of Tokyo Press, Tokyo, Japan, 1984, pp. 287–294.

[17]Legge, H., "Shear Stress and Pressure in Plume Impingement Flow," *Rarefied Gas Dynamics*, edited by V. Boffi and C. Cercignani, Vol. 1, B. G. Teubner, Stuttgart, Germany, 1986, pp. 523–538.

[18]Legge, H., "Plume Impingement Forces on Inclined Flat Plates," *Rarefied Gas Dynamics*, edited by A. Beylich, VCH, Aachen, Germany, 1990, pp. 955–962.

[19]Dettleff, G., "Plume Flows and Plume Impingement in Space Technology," *Progress in Aerospace Sciences*, Vol. 28, 1991, pp. 1–71.

[20]Boyd, I. D., Penko, P. F., Meissner, D. L., and De Witts, K. J., "Experimental and Numerical Investigations of Low-Density Nozzle and Plume Flows of Nitrogen," *AIAA Journal*, Vol. 30, No. 10, 1992, pp. 2453–2460.

[21]Sankovich, V., "Stagnation Pressure Probe for Supersonic Rarefied Gas Dynamics," *Rarefied Gas Dynamics*, edited by V. Boffi and C. Cercignani, Vol. 2, B. G. Teubner, Stuttgart, Germany, 1986, pp. 575–584.

[22]Raju, C., Sreekanth, A. K., and Kurian, J., "Impact Pressure Measurements in High Speed Rarefied Flow," *Mechanics Research Communications*, Vol. 21, No. 2, 1994, pp. 131–138.

[23]Fisher, S. S., and Bharathan, D., "Glow–Discharge Flow Visualization of Low-Density Freejets," *Journal of Spacecrafts and Rockets*, Vol. 10, No. 10, 1973, pp. 658–662.

F. W. Chambers
Associate Editor